Original Research Article

Resolving the Hubble tension with a Late Dark Energy Modification to the ΛCDM Model

ABSTRACT

The Hubble tension arises from the difference between direct measurements of the Hubble constant and indirect measurements based on a cosmological model. This discrepancy has been confirmed with increasing precision, suggesting a potential issue with the current cosmological model. The simplest Lambda Cold Dark Matter (ΛCDM) model, which incorporates a cosmological constant associated with dark energy, provides a good fit for a wide range of cosmological data. In this paper, we propose a modification to the ΛCDM model, hypothesizing that dark energy within gravitationally bound structures does not significantly affect the expansion of space within them. We test this hypothesis by modifying the ΛCDM model accordingly. We simulate this modified ΛCDM model and compare it against both direct and indirect measurements of the Hubble constant. Our results indicate that this modification resolves the Hubble tension, providing a strong fit to both direct and indirect measurements of the Hubble constant.

Keywords: Cosmological constant, Cosmological models, Cosmological parameters, Dark energy, Hubble constant, Hubble tension

1. INTRODUCTION

The increasing precision of cosmological measurements has revealed a discrepancy known as the Hubble tension (see [1] for a review). The Hubble tension refers to the difference between direct measurements of the Hubble constant (H_0) and indirect measurements, given a cosmological model. This tension reaches 5σ between the values obtained using the cosmic microwave background (CMB) data from *Planck* for the Lambda cold dark matter (ΛCDM) model [2] and from the Cepheid-calibrated Type Ia supernovae of the SH0ES project [3].

While systematic errors are considered a possible cause of the tension, the high precision and consistency of the data at both ends — late universe measurements, such as the Cepheid-calibrated Type Ia supernovae, and early universe measurements, such as from the CMB with *Planck* — make this unlikely (for a review of different measurements, see [4]). In particular, for late universe measurements, recent JWST observations provide the strongest evidence that systematic errors in the Hubble Space Telescope Cepheid photometry do not play a significant role in the present Hubble tension [5][6].

Thus, there is growing interest in the possibility that this tension points to a model problem [7]. However, since the simplest ΛCDM model provides a good fit for a large span of cosmological data; therefore, significant alterations are not appropriate.

Fundamentally, the CMB data necessitate that the universe expand by a certain amount so that our current

universe's large-scale clustering of galaxies matches the CMB imprint of the structure after forward extrapolation with the ΛCDM model. This expansion is produced by a ΛCDM model with a Hubble constant H_0 of 67.4 ± 0.5 km s^{-1} Mpc^{-1} [8][9]. On the other hand, direct local measurements employing parallax and extended measurements — for example, using Type Ia supernovae — as far as 10 billion years back are best fitted with a ΛCDM model with an H_0 of 73 ± 1 km s^{-1} Mpc^{-1} [10]. Herein, we will call these two models respectively ΛCDM67 and ΛCDM73.

The cosmological constant, Λ, in the ΛCDM model was added to account for the accelerated expansion of the universe required to fit the late universe measurements of Cepheid-calibrated Type Ia supernovae. Originally proposed by Einstein to keep the universe static, Λ is believed to be due to as yet unknown dark energy in space that has a constant energy density and thus negative pressure, causing space to expand [11]. There is a body of work that attempts to understand how bound structures can affect cosmology and whether the cosmological constant requires modification. However, a consensus has yet to be reached (for example see [12] and [13]). There is also a body of work that has explored modifications to the ΛCDM model, particularly focusing on the dark energy component in the late universe (see [14] for a review). These modifications are now beginning to be tested against data from the DESI collaboration.

In this paper, we explore one such modification and model it to determine if it alleviates the Hubble tension. Our modification is motivated by the question: What if dark energy in space within gravitationally bound structures does not significantly contribute to expansion? At the time the universe was heavily matter dominated, dark energy had a small effect on expansion. Today, it dominates the universe's mass–energy content because it is uniform across space, but within gravitationally bound structures, the density of dark energy is very low, much less than the density of ordinary matter or dark matter [15]; thus, Λ inside these high-gravity objects could be ineffective in contributing to the expansion of space within them.

In this paper, we postulate that the expansion of space within gravitationally bound structures is largely unaffected by the dark energy within them. We then proceed to test this hypothesis by modifying the ΛCDM model accordingly, and we refer to the modified model as the Λ_fCDM model. In the theory section (section 2), we derive a modification of the standard ΛCDM model. In the method section (section 3), we discuss the parameters of the new Λ_fCDM model used to explore its impact on the Hubble tension. In the results section (section 4), we discuss the results of the model runs, from which we draw conclusions.

2. THEORY

The cosmological model was derived from Einstein's field equations; subsequently, a cosmological constant denoted by Λ was introduced. We investigate the modification of the model using Newtonian mechanics because, for an isotropic, spherical, expanding universe, it has been demonstrated that the fundamental aspects of the solution can be comprehended using purely Newtonian dynamics. This is because, in the non-relativistic case (as we employ it well beyond the radiation era), it yields the same Friedmann equation [16]. The objective is to find a modification to the Λ term for use in the normal ΛCDM model. In general relativity, the universe and space expand together; in the Newtonian treatment, we imagine a homogeneous sphere of matter expanding isotropically into existing empty Euclidian space. The sphere has an edge, a center of symmetry, and a fixed mass. The acceleration of the outside edge of the sphere is given by equation (1) [17][18]:

$$\ddot{r} = -\frac{GM}{r^2} = -\frac{G\rho V}{r^2} = -\frac{4\pi G\rho r}{3}, \qquad (1)$$

where G is the gravitational constant, M is the mass of the sphere (which is enclosed in radius r), ρ is the

density, V is the volume of the sphere, and ρr^3 is a constant. To equation (1), a cosmological constant denoted by Λ was added — originally to cancel the gravitational deceleration and make the universe static, and recently to provide a positive acceleration component to the universe, which would become dominant at larger r values, as shown in equation (2):

$$\ddot{r} = -\frac{4\pi G\rho r}{3} + \frac{\Lambda r}{3}. \qquad (2)$$

The physical interpretation of Λ is that it acts on all space and takes the same value at all points in space and time. Although today it dominates the universe's mass–energy content, it is established that within gravitationally bound structures, its effect is minimal. For example, calculations show that within the Coma Cluster, up to a few Mpc radii, dark energy contributes practically nothing compared to the gravitating mass. However, beyond 14 Mpc radii, it quickly becomes dominant again [19]. At the smaller scale of our neighbourhood, dark energy has only a small, albeit measurable, effect on the motion of the Milky Way and Andromeda [20].

Thus, since its contribution is minimal within gravitationally bound structures, it may not assist in expanding that space. Therefore, in these regions, it may not contribute significantly to the expansion of the universe. To test this assumption in our modelling, we will modify the second term in equation 2.

We define V_{GC} as the total volume of bounded structures at any given time (which, as we shall see, is predominantly from galaxy clusters) and V_e as the volume where we postulate lambda is effective (making the simplifying assumption that it has no effect inside gravitationally bounded structures). Then:

$$V_e = V - V_{GC}\ . \qquad (3)$$

Dividing by volume, equation (3) becomes

$$\frac{V_e}{V} = (1 - \frac{V_{GC}}{V}). \qquad (4)$$

We define Λ_{f}, as the effective lambda (without making any change to lambda) in all space excluding gravitationally bound space, and compute it as follows,

$$\Lambda_f = \Lambda\,(1 - \frac{V_{GC}}{V}). \qquad (5)$$

Equation (2) with Λ_{f} substituted for Λ becomes equation (6):

$$\ddot{r} = -\frac{4\pi G\rho r}{3} + \frac{\Lambda_f r}{3}. \qquad (6)$$

We thus utilize the standard ΛCDM model with Λ_{f} instead of Λ (equation 6).

Galaxy clusters are the largest gravitationally bound systems in the universe [21]. Although these clusters presently occupy a small percentage of the universe's volume, they constituted a more substantial fraction in the past when the universe was smaller. Over time, as galaxy clusters formed and expanded, their spatial footprint grew, but several billion years ago, their relative share of the universe began to diminish as their growth rate slowed while the universe continued its expansion. At the outset of cosmic expansion, Λ_{f} equals Λ, given the absence of gravitationally bound structures. However, as the universe evolves, galaxies emerge, followed by the formation of galaxy clusters, causing Λ_{f} to become significantly smaller than Λ. As cluster formation decelerates amid the universe's accelerated expansion, Λ_{f} gradually approaches Λ asymptotically with increasing volume. Throughout this evolutionary process, the number and size of clusters evolve

dynamically. Therefore, in our modeling approach, we numerically integrate the ΛCDM equations with Λ_f substituted for Λ, as described by equation (6). This allows us to characterize the resulting universe using the Λ_fCDM model. We will compute the Hubble parameter *H* from its definition, given by equation (7):

$$H = \frac{\dot{r}}{r} \qquad (7).$$

To achieve a fit to both late and early universe parameters, we will determine the model parameters in the next section.

3. METHOD

In our simulation, we would like to match the Λ_fCDM model to late universe and early universe observations. However, as a proxy for these measurements, we will use their matched ΛCDM models — that is, a ΛCDM67 model for the early universe results and a ΛCDM73 model for the late universe results.

Thus, we create the parameters for the Λ_fCDM model as follows — see Table 1.

Table 1. Universe Simulation Parameters

Parameter for universe	ΛCDM73 (km s^{-1} Mpc^{-1})	ΛCDM67 (km s^{-1} Mpc^{-1})	Λ_fCDM (km s^{-1} Mpc^{-1})	Comments on Λ_fCDM values
Hubble constant H_0	73	67.4	73	Match ΛCDM73 at current time
Critical density	Calculated (from H_0)	Calculated (from H_0)	Same as ΛCDM67	Match ΛCDM67 at early time
Scale factor	Normalized to 10	Scaled to ΛCDM73	Same as ΛCDM67	Match ΛCDM67 stretch
Matter density parameter	0.315	0.315	0.315	Match ΛCDM67 universe at early time
Dark energy density parameter	0.685	0.685	0.685	Match ΛCDM67
Present dark energy	As calculated from above parameters	As calculated from above parameters	Same as for ΛCDM73	Match current ΛCDM73 value
References ΛCDM73	H_0: [22]; densities: [23][24]; some recent results indicate a lower matter density parameter (0.308): [25].			
References ΛCDM67	[23][24]			

Parameters for the Λ_fCDM model are chosen to ensure that the early universe parameters determined by *Planck* remain unchanged, and the total scale factor is chosen to preserve the standard ruler method of calculating the Hubble constant. Thus, to:

a) Preserve the anisotropy of the cosmic microwave background we use parameters that leave the primary anisotropy unchanged by not altering the modeling of effects that occur at the surface of last scattering and before. Specifically, the critical density and the matter density parameters are obtained from the *Planck* results for the ΛCDM67 universe, retaining the early universe conditions.

b) Preserve the secondary anisotropy which occurs between the last scattering surface and today: The total scale factor is matched to the *Planck* data, ensuring the total expansion required to match the current distribution of structure using the standard ruler technique. Additionally, the color temperature of the radiation, which is inversely proportional to the scale length, remains unchanged. Thus, the scale factor (which is arbitrarily normalized to 10 for the ΛCDM73 universe in Table 1) is set to that of the ΛCDM67 universe.

Finally, since we are not focused on the pre-CMB universe, we only model matter and dark energy.

In the late universe, we want Λ_fCDM to behave as ΛCDM73. Thus, the Hubble constant today is set to the value of 73, and we also match the dark energy today to that of ΛCDM73. Note that Λ_fCDM therefore has higher dark energy than the ΛCDM67 universe today and, depending on assumptions about structure formation (as we shall discuss below), lower in earlier times. Also, it is not "flat," although that term is hard to define now that the effective lambda term (Λ_f) is varying over time due to the impact of galaxy clusters.

The above matching maintains a ΛCDM67 early universe and its full-scale factor to the present day, while forcing today's universe to have an H_0 of 73 and a corresponding dark energy value. However, the variation of the scale factor between the last scattering and now differs slightly from what *Planck* assumes. Note that we can pick a lower matter density parameter for ΛCDM73 for the simulation, as its value is not as well established in the references as that from the *Planck* data for ΛCDM67. We will comment on this in the results section (section 4).

In our universe, we must also model gravitationally bounded structure. Let us begin with the current picture. As shown in Table 2, we have estimates for the portion of matter contained in clusters, as well as the mass and size of the clusters. Cluster visible extent is well explored, but gravitationally bound structure extent is much larger because the majority of the cluster mass is in the form of dark matter [26]; we therefore estimate the overall cluster radius from the dark matter halo extent, as it has been found that the Navarro–Frenk–White (NFW) model [27] is an excellent fit to a sample of 50 galaxy clusters at $0.15<z<0.3$ [28]. Note that if the estimate for the portion of matter contained in clusters is lower or higher than we are using, an opposite change in the cluster radius (as the cube root) will yield identical results.

Table 2. Cluster Parameters

Parameter	Value	Comments	References
Density parameter for clusters today Ω_{c0}	0.2		[29]
Cluster mass M_c	$5\text{x}10^{14}$ M_0	Use middle of range of 10^{14} to 10^{15} solar masses.	[30]
Cluster radius, which dictates cluster volume V_c	Fit model at ~4 Mpc	Visible extent 1–5 Mpc. Pick midpoint of 3, or 1.5 for radius. Add dark matter halo extent of gravitational bound structures of 2.5–3x visible radius.	Visible extent: [30] [31] [32] Dark matter halo: [33] NFW general profile: [34] [35]
Portion of space within gravitationally bounded structures today	0.034	Calculated from above values and critical density per Table I. $\frac{V_{GC0}}{V_0} = \Omega_{c0}\ \rho_{crit}\ V_c / M_c$	

With these parameters, we can calculate V_{GC0}/V_0 (where the zero subscript denotes the current value) at a few percent, as shown in the last row of Table 2.

At least for a few billion years back, owing to the stability of clusters, we can calculate V_{GC}/V simply by scaling the current value upwards as the universe shrinks. At earlier times, we also need to take into account changes in the number density and size of clusters.

Simulations with ΛCDM expect the very first stars to emerge some 50–100 million years after the Big Bang and the first galaxies a few hundred million years later, then cosmic mergers take place on progressively larger and larger scales. By the time a few billion years have passed, we expect the universe to be rich in groups and clusters of galaxies, with clusters growing larger, richer, and more evolved as time goes on. About six billion years ago, dark energy became the dominant factor in the expansion of the universe, ensuring a swift drop in cluster growth and in mergers between clusters, leading to a stable cluster population that is not too different from today [36]. However, it is now clear that the predictions of these simulations within ΛCDM for forming stars, galaxies, and clusters are inconsistent with the earlier, evolved structures we are observing with the JWST, a sampling of which is provided in Table 3.

Several studies provide plausible pathways and mechanisms for galaxies to form and grow much more quickly. For example, the most recent simulations that were conducted by Yajima et al. (2022) [37] and Keller et al. (2023) [38].

Table 3. Cluster Development

Event	Time	Observation	References
Early galaxies	After ~200 million years	Detected 87 galaxies that may have been the first to appear in the universe	[39]
Early proto-clusters	z=7.88	JWST early proto-galaxy cluster	[40]
	z∼3.3 (11.8 bya)	A massive proto-supercluster	[41]
Cluster abundance	z∼1.8 (~10 bya)	Detected clusters	[42] [43]
~50% clusters relaxed early	~10 bya	Some clusters are stable starting ~10 bya	[44]
	z=1.16 (~8.5 bya)	Distant, dynamically relaxed, cool core cluster	[45]
	z=1.2 (~8.7 bya)	Evidence of relaxed clusters stable until z=1.2	[46]
Most clusters consistent	To z=1 (~8 bya)	Almost no difference in the X-ray luminosity functions (XLF) for clusters z>0.3 and z<0.3	[47]
		XLF at 0.3<z<0.6 consistent with the local XLF	[48]
		Cluster size does not change significantly in range 0.3<z<0.9	[49] [50]
Cluster number evolution	Constant to z=0.35 (4 bya), ~half to a third by z=0.5 (5.2 bya), drops to ~15% by z=0.7 (6.5 bya)		[51]
	Mild evolution in observed cluster abundance from z=0.5 to 1, half at z=0.5, and 1/6 at z=1		[52]

It is important to clarify that the ΛCDM model does not predict the clustering of the galaxy field directly. Instead, it provides a framework for predicting the density field of the dark matter following epochs of gravitational instability, settling eventually into the dark matter "haloes" [53] that ultimately act as the sites of galaxy formation. As these haloes formed preferentially in locations where the initial density fluctuations were large, they are considered tracers of the underlying density field [54].

Thus, our challenge is that we need the ΛCDM model to estimate clusters at any given time, but we are trying to modify that model because it leads to tensions, not just the Hubble tension, but tensions related to structure formation. Observations of the late universe large-scale structure constrain the strength with which matter is clustered in the universe. These results differ from those inferred by probes of the early universe. This tension, at the level of 2 to 3 σ, is known as the S_8 tension (see [55] for a review). Furthermore, some observations suggest that the formation of large structures took place earlier and was stronger than expected in the ΛCDM model — for example, around z = 0.87, the collision velocity of the interacting galaxy cluster El Gordo and ΛCDM are in tension [56][57].

However, we have some significant larger-scale observations to rely on (the key ones are shown in Table 3). In the last decade or so, owing to the wide-area sky surveys performed with Sunyaev–Zeldovich (SZ) telescopes [58][59][60], it has become possible to detect clusters out to redshifts z ∼1.8 (i.e., 10 billion years ago) with a simpler selection function — namely, the SZ signal tightly correlates with mass [61][62].

Without a definitive timeline for large-scale structure formation, we model two "bookends" for cluster number and size: early cluster and late cluster development; we expect reality to lie somewhere between these two cases. For the early cluster development case, we keep cluster number and size constant to ~8.6 bya, then decrease them linearly to no clusters by ~10 bya. This is motivated by recent observations and modelling described above, and is likely aggressive, but will illustrate the effect of Λ_f clearly. For the late cluster development case, we use *Planck* data for cluster density and keep the size constant. Cluster density is modelled as follows: steady at 1 (times current value) to z = 0.35 (4 bya), decreasing linearly to 0.4 current value at z = 0.53 (5.4 bya), and decreasing linearly to 0.15 at z = 0.7 (6.5 bya) [63], then decreasing linearly to no clusters ~9 bya. The volume occupied by clusters is kept constant since, as shown in Table 3, the clusters are very consistent in size; this is because when early irregular and lumpy cluster shapes grow and become more massive, their radii increase only slowly, as most of the new mass concentrates in the core of the cluster [64]. Thus, in our simulation, we can calculate the volume contained in clusters, V_{GC} , by using the following assumptions: the cluster volume remains constant, the number of clusters varies as specified for both late and early cluster development cases, and the total sphere volume, V, is derived from r. As we perform the numerical integration, we calculate Λ_f at each iteration for both the early and late cluster development cases and incorporate it into equation (6). Tables 1 and 2 provide all other parameters needed for equations (6) and (7).

We do not include any effect of galaxies in our modelling. Approximately 5–10% of galaxies live in gravitationally bound clusters [65] versus alone or in groups. Clusters have hundreds to thousands of galaxies [66]. Thus, for every cluster, there are ~10^4 unbound galaxies, but the cluster radius is 100x the galaxy radius (i.e., Mpc vs. tens of kpc). Thus, the space within galaxies is 1/100^{th} of the space within clusters today, and at z ~1, it is ~1/10^{th} (assuming the cluster number density drops to ~1/10 by z ~1). Galaxies contain a significant proportion of space within them at earlier times, when the universe is much smaller, but at that time, the universe is so matter dominated that small changes in Λ_f do not change the conclusions herein.

4. RESULTS

We integrate equation (6) and use equation (7) to calculate the Hubble parameter *H*. We then plot the scale factor versus time and *H* versus time for both late and early cluster cases within the Λ_fCDM universe. For comparison, we also plot the scale factor and *H* versus time for the ΛCDM73 and ΛCDM67 universes, using equations (2) and (7) along with the parameters provided in Tables 1 and 2. Figure 1 shows the scale factor of the various universe models versus time.

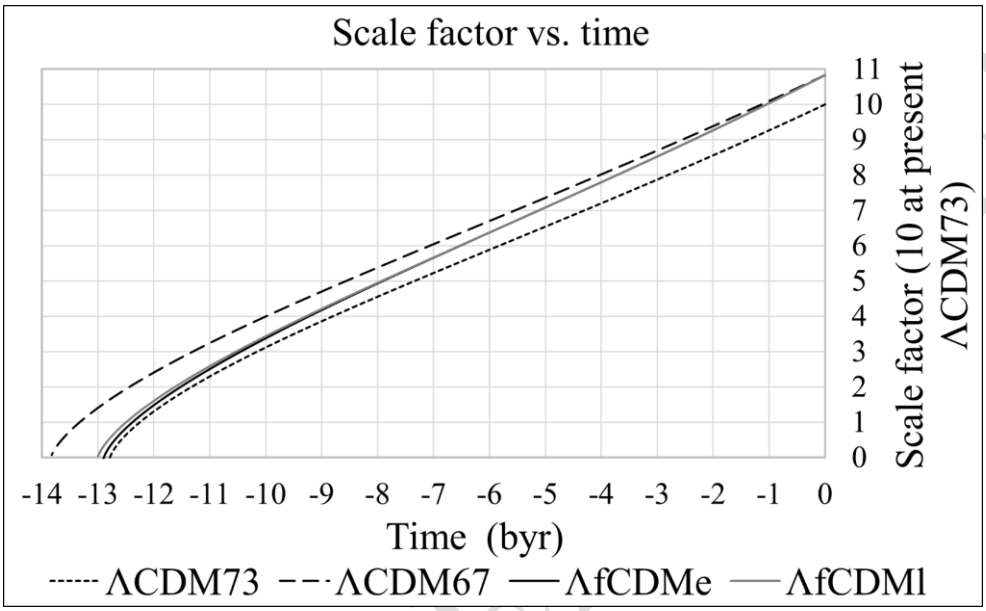

Fig. 1. Scale factor versus time for the various universe models. (Note that the Λ_fCDM models lie virtually on top of each other at this scale, and the grey line hides the black line.)

The Λ_fCDM universes perform as set up (e denotes early cluster development and l denotes late cluster development to distinguish the Λ_fCDM universes). They expand the full-scale factor of the fit to the early universe ΛCDM67 and have the same early scale factor versus time. However, they exhibit a late universe Hubble parameter that matches ΛCDM73 as long as most of the clusters are developed (as we shall see below).

Figure 2 and Figure 3 respectively plot the Hubble parameter versus time and the percent difference between the parameter for the Λ_fCDM universes and ΛCDM73. Note that in Figure 2, the Λ_fCDM universes lie on top of ΛCDM73, except at the far left.

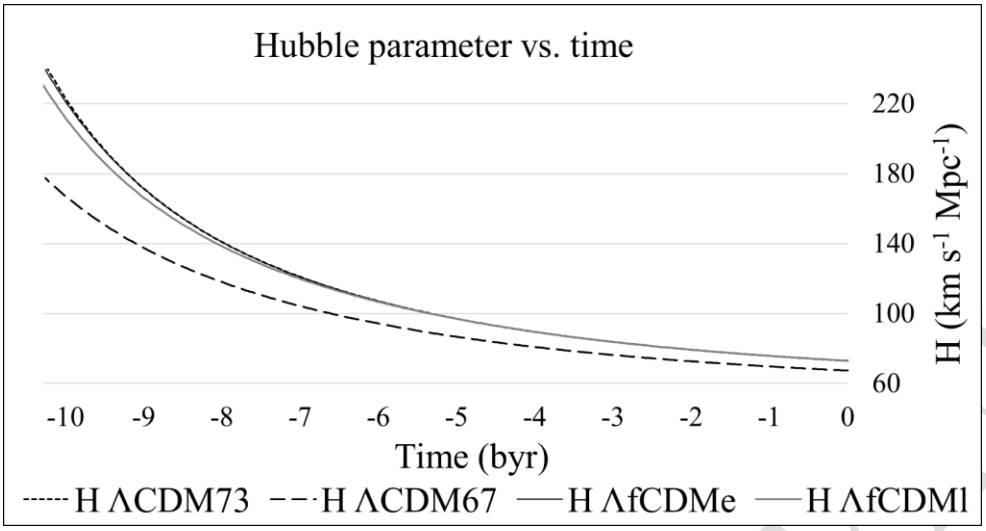

Fig. 2. Hubble parameter *H* vs. time for the various universes.

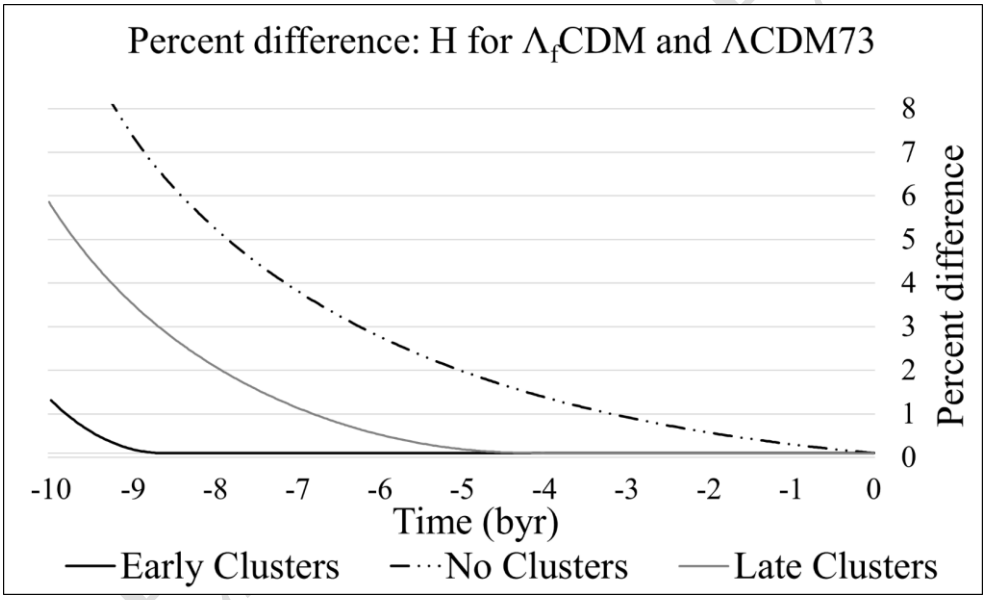

Fig. 3. The difference between *H* for Λ_fCDM and ΛCDM73 universes.

However, the differences are apparent in Figure 3, as clusters disappear back in time. For illustration, the dash-dot curve is for a universe with no clusters. Clearly, the postulate that the expansion of space within gravitationally bound structures is largely unaffected by the dark energy is the cause of the nearly perfect fit. All these graphs are run with the parameters in the prior tables, except the cluster radius is changed to 4.005 Mpc to optimize the fit to H_0=73 km s^{-1} Mpc^{-1} in the late universe.

Figure 4 plots Λ_f (normalized by Λ for the universe with a Hubble constant of 67.4) versus time, as calculated during the numerical integration. This figure illustrates the assumptions regarding cluster development for both the early and late cluster development cases. Note that until about 4 bya (and before about 10 bya), the two lines are coincident.

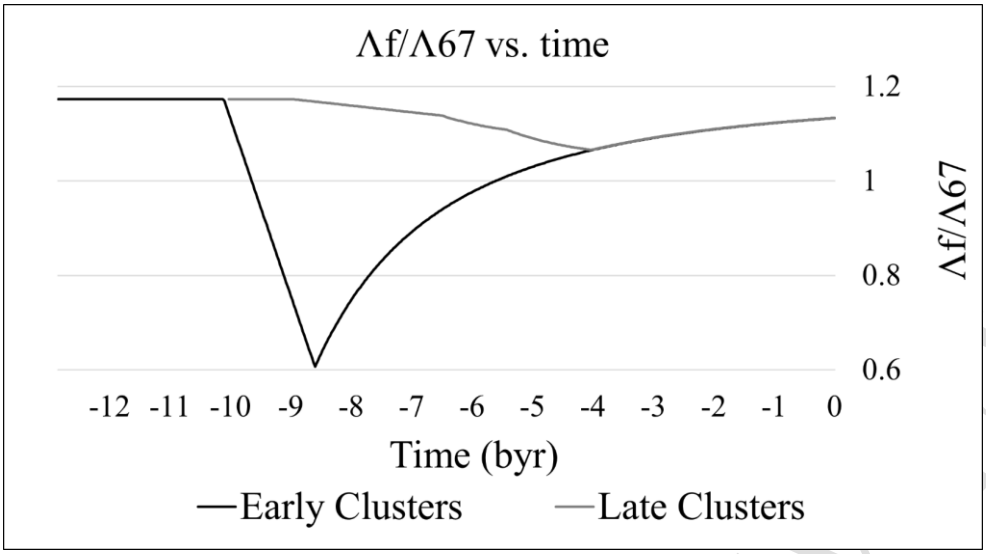

Fig. 4. $\Lambda_f/\Lambda 67$ as clusters develop for early and late cases.

Our bookends in Figure 4 show that the Hubble parameter for the Λ_fCDM universes matches the ΛCDM73 universe in the last 9 byr for the early cluster development case and the last 5 byr for the late cluster development case (see Figure 3). The late cluster development case moves to a lower *H* universe several billion years back (see Figure 2, where the grey curve is leaning towards a lower *H*).

There is some evidence that the inferred value of H_0 vs. redshift isn't constant. A survey of distant quasars gravitationally lensed by closer galaxies calculated the Hubble constant at six different redshift distances. The uncertainties of these values are fairly large, but the inferred value of H_0 for closer lensings seems higher than for more distant lensings [67]. More recently, the DESI Collaboration results have started to offer a clearer understanding of dark energy. Specifically, the best-fit results, which also substantially alleviate the Hubble tension (to just below one sigma), favor a modification known as *w*CDM. This modification to the ΛCDM model assumes that dark energy possesses a constant cosmological equation of state parameter (*w*), representing the ratio of pressure to energy density in the universe. DESI (including CMB data) obtains a value of *w* equal to -1.122 [68], in contrast to the ΛCDM model where *w* is -1. A value of w around -1.12 roughly aligns with the trajectory of the late clusters curve (grey) depicted in Figure 4. This curve starts at (an equivalent *w* of) -1.17, changes to -1.065, and then to -1.133. Additionally, the DESI collaboration investigates a linear time-varying dark energy scenario, where dark energy gets weaker over time. This scenario results in a notable Hubble tension compared to our model, which exhibits weaker and then stronger dark energy and leads to almost no tension.

Finally, the model is robust to other assumptions. The total matter in clusters can be decreased or increased with a cube root adjustment to the cluster radius to yield identical results. The matter density parameter for ΛCDM73 can be reduced from 0.315 and the cluster radius adjusted to obtain a similar fit. For example, a matter density parameter of 0.308 and a cluster radius of 3.8 Mpc obtain the same fit.

5. CONCLUSIONS

Simulations show that a Λ_fCDM model, where Λ is constant, that assumes that dark energy in the space within gravitationally bound structures does not contribute to the expansion of the universe, can resolve the Hubble tension. The almost perfect fit, based on this postulate, provides strong evidence of its correctness. Herein,

we match the new model to the best-fitting ΛCDM models for the early universe and late universe observations. The next step is to fit the actual early and late universe data to the new model based on a structure formation timeline that is also consistent with it.

The Λ_fCDM model for the case where clusters form early (see Figure 4, early clusters case and many other possible scenarios between the early and late cluster curves) implies that as structure formation gets going, there is a positive feedback mechanism. That same structure diminishes the effect of Λ (i.e., Λ_f is less than Λ), allowing for enhanced structure formation. Thus, more structure forms faster and earlier than in the traditional ΛCDM. However, this situation reverses as Λ becomes more dominant and larger (i.e., Λ_f is greater than Λ) by 5 billion years ago. From then on, the universe experiences a more accelerated expansion. This should lead to a more homogeneous universe locally than predicted with the CMB data from *Planck* and the standard ΛCDM (without the need to change the matter density parameter), which is moving in the right direction to resolve the S_8 tension [69]. Around z of 0.87, the enhanced structure formation compared to the ΛCDM67 model (due to Λ_f being lower than Λ in early clusters case in Figure 4 at ~7.3 bya) should also help resolve the tension between the existence of El Gordo and Λ_fCDM [70][71]. To confirm and quantify the reduction or elimination of the S_8 tension and the El Gordo tension with the Λ_fCDM model, one needs to run a cosmological simulation of the model.

Finally, any universe that attempts to fit a H_0 of 73 km s^{-1} Mpc^{-1}, even for part of its age, will have a shorter age than implied by the *Planck* data, which fit a H_0 of 67.4 km s^{-1} Mpc^{-1}. Thus, the model herein, although leading to an older age of the universe than a standard ΛCDM73, still has an age of about 13 billion years, with different parameter assumptions (such as a lower matter density parameter of 0.308), making it older by ~100 million years.

STATEMENTS AND DECLARATIONS

Code Availability statement: the manuscript has no associated code/software.

Data Access Statement: The data underlying this article were obtained from public domain sources referenced herein.

REFERENCES

[1] E. Abdalla et al., Cosmology intertwined: A review of the particle physics, astrophysics, and cosmology associated with the cosmological tensions and anomalies, JHEAp. 34 (2022) 49-211. https://doi.org/10.1016/j.jheap.2022.04.002.

[2] *Planck* Collaboration et al., 2020. *Planck* 2018 results, VI. Cosmological parameters. A&A. 641, A6. https://doi.org/10.1051/0004-6361/201833910.

[3] A.G. Riess et al., 2022. A Comprehensive Measurement of the Local Value of the Hubble Constant with 1 km s−1 Mpc−1 Uncertainty from the Hubble Space Telescope and the SH0ES Team. ApJL. 934, L7. https://doi.org/10.3847/2041-8213/ac5c5b

[4] E. Abdalla et al., Cosmology intertwined: A review of the particle physics, astrophysics, and cosmology associated with the cosmological tensions and anomalies, JHEAp. 34 (2022) 49-211. https://doi.org/10.1016/j.jheap.2022.04.002.

[5] A.G. Riess et al., 2023. Crowded No More: The Accuracy of the Hubble Constant Tested with High-resolution Observations of Cepheids by JWST. ApJL. 956, L18. https://doi.org/10.3847/2041-8213/acf769
[6] A.G. Riess et al., 2024. JWST Observations Reject Unrecognized Crowding of Cepheid Photometry as an Explanation for the Hubble Tension at 8σ Confidence. ApJL. 962, L17. https://doi.org/10.3847/2041-8213/ad1ddd
[7] E. Abdalla et al., Cosmology intertwined: A review of the particle physics, astrophysics, and cosmology associated with the cosmological tensions and anomalies, JHEAp. 34 (2022) 49-211. https://doi.org/10.1016/j.jheap.2022.04.002.
[8] Planck Collaboration et al., 2020. *Planck* 2018 results, VI. Cosmological parameters. A&A. 641, A6. https://doi.org/10.1051/0004-6361/201833910.
[9] Planck Collaboration et al., 2021. *Planck* 2018 results, VI. Cosmological parameters (Corrigendum). A&A. 652, C4, https://doi.org/10.1051/0004-6361/201833910e.
[10] A.G. Riess et al., 2022. A Comprehensive Measurement of the Local Value of the Hubble Constant with 1 km s−1 Mpc−1 Uncertainty from the Hubble Space Telescope and the SH0ES Team. ApJL. 934, L7. https://doi.org/10.3847/2041-8213/ac5c5b.
[11] B. Ryden, Introduction to Cosmology, 2nd ed., Cambridge Univ. Press, Cambridge, UK, 2018, p. 66.
[12] S. Sikora, K. Głód, 2021. Construction of the cosmological model with periodically distributed inhomogeneities with growing amplitude. Eur. Phys. J. C81, 208. https://doi.org/10.1140/epjc/s10052-021-08992-2.
[13] T. Buchert et al., Is there proof that backreaction of inhomogeneities is irrelevant in cosmology? Class. Quantum Grav. 32 (2015) 215021. https://doi.org/10.48550/arXiv.1505.07800.
[14] E. Di Valentino et al., In the realm of the Hubble tension—a review of solutions, Class. Quantum Grav. 38 (2021) 153001. https://doi.org/10.1088/1361-6382/ac086d.
[15] Steinhardt P.J., Turok N., 2006. Why the Cosmological Constant Is Small and Positive. Science. 312, 5777, pp.1180. https://doi.org/10.1126/science.1126231
[16] B. Ryden, Introduction to Cosmology, 2nd ed., Cambridge Univ. Press, Cambridge, UK, 2018, Ch. 4-5.
[17] B. Ryden, Introduction to Cosmology, 2nd ed., Cambridge Univ. Press, Cambridge, UK, 2018, p. 53.
[18] E. Harrison, Cosmology: The Science of the Universe., Cambridge Univ. Press, Cambridge, UK, 2000, p. 331.
[19] A.D. Chernin et al., 2013. Dark energy and the structure of the Coma cluster of galaxies. A&A. 553, A101. https://doi.org/10.1051/0004-6361/201220781.
[20] D. Benisty, A. Davis, N. Wyn Evans, 2023. Constraining Dark Energy from the Local Group Dynamics. ApJL. 953, L2. https://doi.org/10.3847/2041-8213/ace90b.
[21] T. Hong, J.L. Han, Z.L. Wen, 2016. A Detection Of Baryon Acoustic Oscillations From The Distribution Of Galaxy Clusters. ApJ. 826, 154, https://doi.org/10.3847/0004-637X/826/2/154.
[22] A.G. Riess et al., 2022. A Comprehensive Measurement of the Local Value of the Hubble Constant with 1 km s^{-1} Mpc^{-1} Uncertainty from the Hubble Space Telescope and the SH0ES Team. ApJL. 934, L7. https://doi.org/10.3847/2041-8213/ac5c5b.
[23] *Planck* Collaboration et al., 2020. *Planck* 2018 results, VI. Cosmological parameters. A&A. 641, A6. https://doi.org/10.1051/0004-6361/201833910.
[24] *Planck* Collaboration et al., 2021. *Planck* 2018 results, VI. Cosmological parameters (Corrigendum). A&A. 652, C4. https://doi.org/10.1051/0004-6361/201833910e.

[25] M.G. Dainotti et al, 2021. On the Hubble Constant Tension in the SNe Ia Pantheon Sample. ApJ. 912, 150. https://doi.org/10.3847/1538-4357/abeb73.
[26] A.H. Gonzalez et al, 2013. Galaxy Cluster Baryon Fractions Revisited. ApJ. 778, 14. https://doi.org/10.1088/0004-637X/778/1/14.
[27] J.F. Navarro, C.S. Frenk, S.D.M. White, 1997. A Universal Density Profile from Hierarchical Clustering. ApJ. 490, 493. https://doi.org/10.1086/304888.
[28] N. Okabe et al, 2013. LoCuSS: The Mass Density Profile Of Massive Galaxy Clusters At $z = 0.2$. ApJL. 769, L35. https://doi.org/10.1088/2041-8205/769/2/L35.
[29] B. Ryden, Introduction to Cosmology, 2nd ed., Cambridge Univ. Press, Cambridge, UK, 2018, p. 135.
[30] K.R. Lang, The Life and Death of Stars, Cambridge Univ. Press, Cambridge, UK, 2013, p. 279.
[31] B. Ryden, Introduction to Cosmology, 2nd ed., Cambridge Univ. Press, Cambridge, UK, 2018, p. 134.
[32] S. White, 2015. Cluster Cosmology: A Theoretical View. RAS Discussion Meeting (London), wwwmpa.mpa-garching.mpg.de/~swhite/talk/RAS_clusters15.pdf.
[33] L.S. Sparke, J.S. Gallagher, Galaxies in the Universe, 2nd ed., Cambridge Univ. Press, Cambridge, UK, 2007, pp. 26-28.
[34] J.F. Navarro et al, 1997. A Universal Density Profile from Hierarchical Clustering. ApJ. 490, 493. https://doi.org/10.1086/304888.
[35] N. Okabe et al, 2013. LoCuSS: The Mass Density Profile Of Massive Galaxy Clusters At $z = 0.2$. ApJL. 769, L35. https://doi.org/10.1088/2041-8205/769/2/L35.
[36] B. Ryden, Introduction to Cosmology, 2nd ed., Cambridge Univ. Press, Cambridge, UK, 2018, Ch. 11.
[37] H. Yajima et al., 2022. FOREVER22: galaxy formation in protocluster regions. MNRAS, 509, 3, pp. 4037–4057, https://doi.org/10.1093/mnras/stab3092.
[38] B.W. Keller et al, 2023. Can Cosmological Simulations Reproduce the Spectroscopically Confirmed Galaxies Seen at $z \geq 10$? ApJL. 943, L28. https://doi.org/10.3847/2041-8213/acb148.
[39] H. Yan et al, 2023. First Batch of $z \approx 11$–20 Candidate Objects Revealed by the James Webb Space Telescope Early Release Observations on SMACS 0723-73. ApJL. 942, L9. https://doi.org/10.3847/2041-8213/aca80c.
[40] T. Morishita et al., 2023. Early Results from GLASS-JWST. XIV. A Spectroscopically Confirmed Protocluster 650 Million Years after the Big Bang. ApJL. 947, L24. https://doi.org/10.3847/2041-8213/acb99e.
[41] B. Forrest et al., 2023. Elentári: a massive proto-supercluster at $Z \sim 3.3$ in the COSMOS field. MNRAS Letters. 526, L56-62. https://doi.org/10.1093/mnrasl/slad114.
[42] *Planck* Collaboration et al., 2014. *Planck* 2013 results, XX. Cosmology from Sunyaev–Zeldovich cluster counts. A&A. 571, A20. https://doi.org/10.1051/0004-6361/201321521.
[43] V. Ghirardini et al., 2021. Evolution of the Thermodynamic Properties of Clusters of Galaxies out to Redshift of 1. ApJ. 910, 14. https://doi.org/10.3847/1538-4357/abc68d.
[44] M. McDonald, Galaxy Cluster Evolution Over the Past 10 Billion Years, Center for Astrophysics, Harvard & Smithsonian, Cambridge, MA, 2017.
[45] M.S. Calzadilla et al., 2023. SPT-CL J2215−3537: A Massive Starburst at the Center of the Most Distant Relaxed Galaxy Cluster. ApJ. 947, 44. https://doi.org/10.3847/1538-4357/acc6c2.
[46] E. Darragh-Ford et al, 2023, The Concentration–Mass relation of massive, dynamically relaxed galaxy clusters: agreement between observations and ΛCDM simulations. MNRAS. 521, 1, pp. 790-799. https://doi.org/10.1093/mnras/stad585.

[47] A.D. Lewis et al, 2002. New X-Ray Clusters in the *Einstein* Extended Medium-Sensitivity Survey. I. Modifications to the X-Ray Luminosity Function. ApJ. 566, 2, p.744. https://doi.org/10.1086/324139.
[48] S.C. Ellis, L.R. Jones, 2002. A reanalysis of the X-ray luminosities of clusters of galaxies with $0.3<z<0.6$ in the EMSS sample. MNRAS. 330, 3, pp. 631-64. https://doi.org/10.1046/j.1365-8711.2002.05092.x.
[49] G. Khullar et al., 2022. Synthesizing Stellar Populations in South Pole Telescope Galaxy Clusters. I. Ages of Quiescent Member Galaxies at $0.3 < z < 1.4$. ApJ. 934, 177. https://doi.org/10.3847/1538-4357/ac7c0c.
[50] A. Muzzin et al., 2012. The Gemini Cluster Astrophysics Spectroscopic Survey (GCLASS): The Role of Environment and Self-Regulation in Galaxy Evolution at $z \sim 1$. ApJ. 746, 188. https://doi.org/10.1088/0004-637X/746/2/188.
[51] *Planck* Collaboration et al., 2016. *Planck* 2015 results, XXIV. Cosmology from Sunyaev-Zeldovich cluster counts. A&A. 594, A24. https://doi.org/10.1051/0004-6361/201525833.
[52] White S., 2015. Cluster Cosmology: A Theoretical View. RAS Discussion Meeting (London), wwwmpa.mpa-garching.mpg.de/~swhite/talk/RAS_clusters15.pdf
[53] J.F. Navarro et al, 1997. A Universal Density Profile from Hierarchical Clustering. ApJ. 490, 493. https://doi.org/10.1086/304888.
[54] C. Hernández-Aguayo et al., 2023. The MillenniumTNG Project: high-precision predictions for matter clustering and halo statistics. MNRAS. 524, 2, pp. 2556–2578. https://doi.org/10.1093/mnras/stad1657.
[55] Abdalla E. et al., Cosmology intertwined: A review of the particle physics, astrophysics, and cosmology associated with the cosmological tensions and anomalies, JHEAp, 34 (2022) 49-211. https://doi.org/10.1016/j.jheap.2022.04.002.
[56] E. Asencio et al, 2021. A massive blow for ΛCDM – the high redshift, mass, and collision velocity of the interacting galaxy cluster El Gordo contradicts concordance cosmology. MNRAS. 500, 4, pp. 5249-5267. https://doi.org/10.1093/mnras/staa3441.
[57] E. Asencio et al, 2023. The El Gordo Galaxy Cluster Challenges ΛCDM for Any Plausible Collision Velocity. ApJ. 954, 162. https://doi.org/10.3847/1538-4357/ace62a.
[58] J.E. Carlstrom et al., 2011. The 10 Meter South Pole Telescope. PASP. 123, 568. https://doi.org/10.1086/659879.
[59] J.W. Fowler et al., 2007. Optical design of the Atacama Cosmology Telescope and the Millimetre Bolometric Array Camera. Appl. Opt.. 46, pp. 3444-3454. https://doi.org/10.1364/AO.46.003444.
[60] *Planck* Collaboration et al., 2016. *Planck* 2015 results, XIII. Cosmological parameters. A&A. 594, A13. https://doi.org/10.1051/0004-6361/201525830.
[61] S. Bocquet et al., 2019. Cluster Cosmology Constraints from the 2500 deg^2 SPT-SZ Survey: Inclusion of Weak Gravitational Lensing Data from Magellan and the Hubble Space Telescope. ApJ. 878, 55. https://doi.org/10.3847/1538-4357/ab1f10.
[62] *Planck* Collaboration et al., 2014. *Planck* 2013 results, XX. Cosmology from Sunyaev–Zeldovich cluster counts. A&A, 571, A20. https://doi.org/10.1051/0004-6361/201321521
[63] *Planck* Collaboration et al., 2016. *Planck* 2015 results, XIII. Cosmological parameters. A&A. 594, A13. https://doi.org/10.1051/0004-6361/201525830.
[64] L.S. Sparke, J.S. Gallagher, Galaxies in the Universe, 2nd ed., Cambridge Univ. Press, Cambridge, UK, 2007, p. 294.

[65] L.S. Sparke, J.S. Gallagher, Galaxies in the Universe, 2nd ed., Cambridge Univ. Press, Cambridge, UK, 2007, p. 292.
[66] K.R. Lang, The Life and Death of Stars, Cambridge Univ. Press, Cambridge, UK, 2013, p. 279.
[67] K.C. Wong et al., 2020. H0LiCOW – XIII. A 2.4 per cent measurement of H_0 from lensed quasars: 5.3σ tension between early- and late-Universe probes. MNRAS. 498, pp. 1420-1439. https://doi.org/10.1093/mnras/stz3094.
[68] DESI Collaboration et al., 2024. DESI 2024 VI: Cosmological Constraints from the Measurements of Baryon Acoustic Oscillations. https://arXiv:2404.03002, Table 10.
[69] H. Zohren et al., 2022. Extending empirical constraints on the SZ–mass scaling relation to higher redshifts via HST weak lensing measurements of nine clusters from the SPT-SZ survey at $z \gtrsim 1$. A&A. 668, A18. https://doi.org/10.1051/0004-6361/202142991.
[70] E. Asencio et al, 2021. A massive blow for ΛCDM – the high redshift, mass, and collision velocity of the interacting galaxy cluster El Gordo contradicts concordance cosmology. MNRAS. 500, 4. https://doi.org/10.1093/mnras/staa3441.
[71] E. Asencio et al, 2023. The El Gordo Galaxy Cluster Challenges ΛCDM for Any Plausible Collision Velocity. ApJ. 954, 162. https://doi.org/10.3847/1538-4357/ace62a.